




Research Article

Efficiency at Maximum Power in a Parallel Connected Two Quantum Dots Heat Engine

Tibebe Birhanu ¹, Yigermal Bassie ², Yoseph Abebe ³ and Mulugeta Bekele⁴

¹Department of Physics, University of Gondar, Gondar, Ethiopia

²Department of Physics, Wolkite University, Wolkite, Ethiopia

³Department of Physics, Debre Markos University, Debre Markos, Ethiopia

⁴Department of Physics, Addis Ababa University, Addis Ababa, Ethiopia

Correspondence should be addressed to Tibebe Birhanu; tibebebirhanu@gmail.com

Received 10 February 2023; Revised 17 May 2023; Accepted 29 May 2023; Published 3 June 2023

Academic Editor: Natt Makul

Copyright © 2023 Tibebe Birhanu et al. This is an open access article distributed under the Creative Commons Attribution License, which permits unrestricted use, distribution, and reproduction in any medium, provided the original work is properly cited.

In this paper, we proposed a model in which a single level of two quantum dots is connected in parallel and embedded between two leads with different temperatures and chemical potentials. The temperature and chemical potential gradient help the electron flow cyclically and act as a heat engine. We explore the thermodynamic properties of the model such as heat flux and power as a function of dot energy. We also carried out analytical and numerical solutions for efficiency at maximum power of the thermoelectric engine. The resulting efficiency of our engine agrees with the Curzon–Ahlborn expression up to quadratic terms in Carnot efficiency.

1. Introduction

The concept of thermodynamics has been developed from the analysis of heat engines' performance. Carnot invented an idealized mathematical model of heat engines called the Carnot cycle and proved that there exists a maximum efficiency of all heat engines, which is given by Carnot efficiency. This efficiency is a central cornerstone of thermodynamics. It states that a reversible Carnot engine's efficiency attains the maximum possible work for a given temperature of the hot (T_h) and cold (T_c) reservoirs but generates zero power because it is an infinitely slow operation. The efficiency ($\eta_c = 1 - T_c/T_h$) of the Carnot cycle is the upper bound on the efficiency at which real heat engines are unrealistically high. The practical implications are more limited since the upper limit η_c is only reached for reversible engine. One of the important questions is what will be the efficiency at maximum power of a system that operates in finite time. In a groundbreaking work, Curzon and Ahlborn [1] obtained this efficiency for the Carnot engine by

optimizing the Carnot cycle with respect to power rather than efficiency, which is given by Curzon–Ahlborn efficiency, η_{CA}

$$\eta_{CA} = 1 - \sqrt{\frac{T_c}{T_h}} = \frac{\eta_c}{2} + \frac{\eta_c^2}{8} + \mathcal{O}(\eta_c^3). \quad (1)$$

This efficiency is used to seek a more realistic upper bound on the efficiency of a heat engine in the endoreversible approximation [1, 2] (taking into account the dissipation only in the heat transfer process). Currently, it has been shown that the Curzon–Ahlborn efficiency is an exact consequence of linear irreversible thermodynamics when operating under conditions of strong coupling between the heat flux and the work [3–5]. The value of 1/2 for the linear coefficient in equation (1) is therefore universal for such systems. Furthermore, the diverse system in nature has been found investigating efficiency at maximum power such as Brownian particle undergoing a Carnot cycle through the

modulation of a harmonic potential [6], Feynman Ratchet and Powl model [7], and quantum dots connected in two leads with different temperatures and chemical potential [8]. The result of efficiency at maximum power for all models mentioned previously agreed up to quadratic order in η_c .

In thermoelectricity devices, the phenomena of the Seebeck effect, Peltier effect, and Thomson effect have been described by the temperature or potential difference. Snyder and Toberer [9] have discovered the thermoelectric material with significantly higher thermodynamic yields in the early 1990s. The development in the field of nanostructured materials is particularly intriguing [10]. Since then, thermoelectric experiments on silicon nanowires [11], individual carbon nanotubes [12], and molecular junctions [13] have been reported. Such thermoelectric devices can be used as an energy converter, i.e., heat to work. In particular, Humphrey et al. [14, 15] reported that Carnot efficiency could be reached for electron transport between two leads at different temperatures and chemical potentials, by connecting them through a channel sharply tuned at the energy for which the electron density is the same in both leads.

Recently, a tiny heat engine (with a single level quantum dots) in contact with hot and cold heat reservoirs with different chemical potentials has been proposed by Esposito et al. [8]. They studied how the device operates and determined the efficiency at maximum power and compared their value with that of the Curzon–Ahlborn efficiency. Besides, the thermoelectric properties of two quantum dots connected in parallel have been studied in Reference [16].

In this paper, we introduce a detailed thermodynamic analysis of electron transport through parallelly connected two identical quantum dots connecting two leads at different temperatures and chemical potentials. Due to the temperature gradient, the electrons transport from hot lead to cold lead through a dot; in contrast, electrons transport from cold lead to hot lead through a dot due to chemical potential. The temperature and chemical potential gradient cause the electron transport through quantum dots to act as a thermoelectric engine.

The rest of this paper is organized as follows: in Section 2, the model is introduced and thermodynamic quantities are determined. Section 3 evaluates and explores the behaviors of heat flux and power as a function of energy parameter, a scaled Δ/ϵ characterizing the energy difference between the two levels. In Section 4, we evaluate the efficiency at maximum power by using a perturbation solution and numerical solution, and the result that we get for the efficiency at maximum power lies between the Carnot efficiency and Curzon–Ahlborn efficiency. In Section 5, we summarize and conclude.

2. The Model and Derivation of the Thermodynamic Quantities

We consider a model that is two quantum dots parallelly connected into hot and cold reservoirs of temperatures T_r and T_l and chemical potentials μ_r and μ_l , respectively, as shown in Figure 1. Due to their size variation, the quantum dots have different single energy levels associated with each

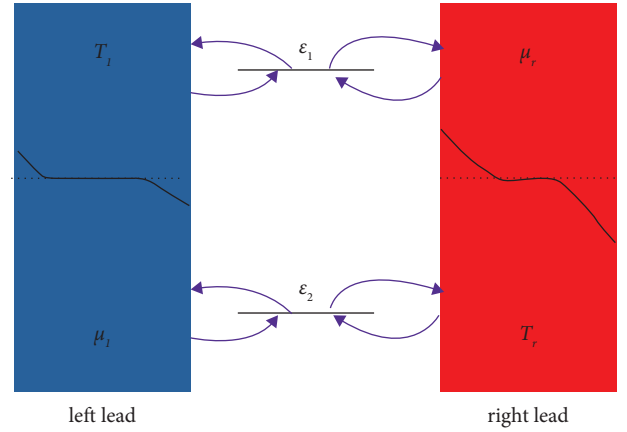


FIGURE 1: Sketch of nanothermoelectric engine consisting of two quantum dots embedded between two leads at different temperatures and chemical potentials. We choose by convention $T_l < T_r$.

of them. Accordingly, we consider the single energy level of the first quantum dot ϵ_1 to be $\epsilon + \Delta$, while that of the second quantum dot ϵ_2 has to be $\epsilon - \Delta$.

We assume that the electrons thermalize instantaneously to the temperature of the leads upon tunnelling to the reservoirs and the electron transports through quantum dots with a sharply defined energy. If the level remains occupied by an electron while it is lowered (raised), power is extracted from (injected into) the system, $W < 0$ ($W > 0$), respectively. If the level remains empty while energy changes, neither power nor heat flux is produced. When the empty (filled) level at energy $\epsilon + \Delta$ and $\epsilon - \Delta$ is filled (emptied) by an electron, an amount of heat flux Q_r (Q_l) enters the system, respectively.

The dots with energy levels $\epsilon + \Delta$ and $\epsilon - \Delta$ exchange electrons with leads as shown in Figure 1. The quantum dot is either empty (state 1) or filled (state 2) for the first quantum dot and the second quantum dot either empty (state 3) or filled (state 4). The crucial variables of the problem are the scaled energy barriers with ($k_B = 1$) of the first and second quantum dots, respectively, which are given by

$$\begin{aligned} x_v &= \frac{\epsilon + \Delta - \mu_v}{T_v}, \\ y_v &= \frac{\epsilon - \Delta - \mu_v}{T_v}, \end{aligned} \quad (2)$$

where $v = l, r$

The master equation [17–19] describes the probabilities of the dots being in a particular state change in time as

$$\begin{aligned} \begin{pmatrix} \dot{P}_1(t) \\ \dot{P}_2(t) \end{pmatrix} &= \begin{pmatrix} -W_{21} & W_{12} \\ W_{21} & -W_{12} \end{pmatrix} \begin{pmatrix} P_1(t) \\ P_2(t) \end{pmatrix}, \\ \begin{pmatrix} \dot{P}_3(t) \\ \dot{P}_4(t) \end{pmatrix} &= \begin{pmatrix} -W_{43} & W_{34} \\ W_{43} & -W_{34} \end{pmatrix} \begin{pmatrix} P_3(t) \\ P_4(t) \end{pmatrix}, \end{aligned} \quad (3)$$

where P_1, P_2, P_3 , and P_4 are the probability of the quantum dots in state 1, state 2, state 3, and state 4, respectively.

Here, the transitional rate in the first quantum dot is given by

$$\begin{aligned} W_{12} &= \sum_{\nu=l,r} W_{12}^{(\nu)} = \sum_{\nu=l,r} a_{\nu}(1 - f_{\nu}), \\ W_{21} &= \sum_{\nu=l,r} W_{21}^{(\nu)} = \sum_{\nu=l,r} a_{\nu}(f_{\nu}), \end{aligned} \quad (4)$$

and the transitional rates in the second quantum dot are given by

$$\begin{aligned} W_{34} &= \sum_{\nu=l,r} W_{34}^{(\nu)} = \sum_{\nu=l,r} b_{\nu}(1 - g_{\nu}), \\ W_{43} &= \sum_{\nu=l,r} W_{43}^{(\nu)} = \sum_{\nu=l,r} b_{\nu}(g_{\nu}). \end{aligned} \quad (5)$$

Here, a_{ν} and b_{ν} are the Einstein coefficients which are independent of the dots' energy and f_{ν} and g_{ν} are the Fermi distributions given by

$$\begin{aligned} f_{\nu} &= [\exp(x_{\nu}) + 1]^{-1}, \\ g_{\nu} &= [\exp(y_{\nu}) + 1]^{-1}. \end{aligned} \quad (6)$$

In this paper, we focus on the steady state properties of the device. The steady state distributions for both dots' occupation follow from $W_{21(43)}P_{1(3)}^{\text{ss}} = W_{12(34)}P_{2(4)}^{\text{ss}}$ with $P_{1(3)}^{\text{ss}} + P_{2(4)}^{\text{ss}} = 1$. The resulting probability current from the lead ν to the first and second dot is

$$\begin{aligned} I_{\nu} &= W_{21}^{\nu}P_1^{\text{ss}} - W_{12}^{\nu}P_2^{\text{ss}}, \\ J_{\nu} &= W_{43}^{\nu}P_3^{\text{ss}} - W_{34}^{\nu}P_4^{\text{ss}}, \end{aligned} \quad (7)$$

respectively. Using $I_r = -I_l$, $J_r = -J_l$, $W_{12} + W_{21} = a_r + a_l$, and $W_{34} + W_{43} = b_r + b_l$, we can rewrite the result for the flux from the right lead as

$$\begin{aligned} I_r &= \alpha(f_r - f_l), \\ J_r &= \gamma(g_r - g_l), \end{aligned} \quad (8)$$

where $\alpha = (a_r a_l)/(a_r + a_l)$ and $\gamma = (b_r b_l)/(b_r + b_l)$. Equation (8) is the Landauer formula for a single infinitely sharp resonance (i.e., without broadening). The steady state heat per unit time for the first quantum dot \dot{Q}_r' and the second quantum dot \dot{Q}_r'' extracted from the lead r is, respectively, given by

$$\begin{aligned} \dot{Q}_r' &= (\epsilon + \Delta - \mu_r)I_r = \alpha T_r x_r (f_r - f_l), \\ \dot{Q}_r'' &= (\epsilon - \Delta - \mu_r)J_r = \alpha T_r y_r (g_r - g_l). \end{aligned} \quad (9)$$

The total heat flux enters into the quantum dots from lead r .

$$\dot{Q}_r = \dot{Q}_r' + \dot{Q}_r'' = \alpha T_r [x_r (f_r - f_l) + y_r (g_r - g_l)]. \quad (10)$$

The net power output by both quantum dots is the sum of the total heat flux getting into it and dissipates cold into cold reservoir which is given by

$$\begin{aligned} \dot{W} &= \alpha T_r [x_r (f_r - f_l) + y_r (g_r - g_l)] \\ &\quad + \alpha T_l [x_l (f_r - f_l) + y_l (g_r - g_l)]. \end{aligned} \quad (11)$$

The corresponding thermodynamic efficiency reads

$$\begin{aligned} \eta &= \frac{W}{Q_r} = \frac{\dot{W}}{\dot{Q}_r} \\ &= \frac{(f_r - f_l)[x_r - (1 - \eta_c)x_l] + (g_r - g_l)[y_r - (1 - \eta_c)y_l]}{x_r(f_r - f_l) + y_r(g_r - g_l)}. \end{aligned} \quad (12)$$

The entropy production associated with the master equation (3) is given as follows [20–23] for the first quantum dot:

$$\sigma_1 = \sum_{i,j,\nu} W_{ij}^{\nu} P_j^{\text{ss}} \ln \frac{W_{ij}^{\nu} P_j^{\text{ss}}}{W_{ji}^{\nu} P_i^{\text{ss}}}, \quad (13)$$

where $i, j = 1, 2$. Noting that $\ln W_{12}/W_{21} = x_r$, one finds, in agreement with standard irreversible thermodynamics [19], the following expression for the entropy production:

$$\sigma_1 = F_m J_m - F_e J_e = \alpha(x_l - x_r)(f_r - f_l) \geq 0. \quad (14)$$

Thermodynamics forces for matter and energy flow, F_m and F_e , are given by

$$F_m \equiv \left(\frac{\mu_r}{T_r} \right), F_e \equiv \frac{1}{T_r} - \frac{1}{T_l}. \quad (15)$$

We stress that the corresponding matter and heat flow are given by

$$J_m = -I_r, J_e = -(\epsilon + \Delta)I_r. \quad (16)$$

In the same spirit, the entropy production, thermodynamics forces for matter and energy flow, and their corresponding matter and flow of the second quantum dot can be expressed as

$$\sigma_2 = K_m R_m - K_e R_e = \alpha(y_l - y_r)(g_r - g_l) \geq 0, \quad (17)$$

$$K_m \equiv -\left(\frac{\mu_r}{T_r} \right), K_e \equiv \frac{1}{T_r} - \frac{1}{T_l}, \quad (18)$$

$$R_m = -J_r, R_e = -(\epsilon - \Delta)J_r, \quad (19)$$

respectively.

The matter and heat flow are perfectly coupled and the condition for attaining both Carnot and Curzon–Ahlborn efficiency, namely, that the determinant of the corresponding Onsager matrix be zero, is fulfilled [1, 24].

Likewise [8], we first discuss the case of equilibrium. It can control thermodynamic quantities by controlling the current because of the perfect coupling. Under this condition, detailed balance is valid, $I_{\nu} = 0$ and $J_{\nu} = 0$, valid if and only if $f_l = f_r$, $g_l = g_r$ or equivalently, $x_l = x_r$, $y_l = y_r$. The efficiency and the entropy production then become equal to the Carnot efficiency, cf. equation (12), and vanishes (cf. equation (13) and cf. equation (17)), respectively. We note that $x_l = x_r$, $y_l = y_r$ do not require that the thermodynamic forces F_m and F_e vanish separately, i.e., this singular balancing point equilibrium does not require temperature and

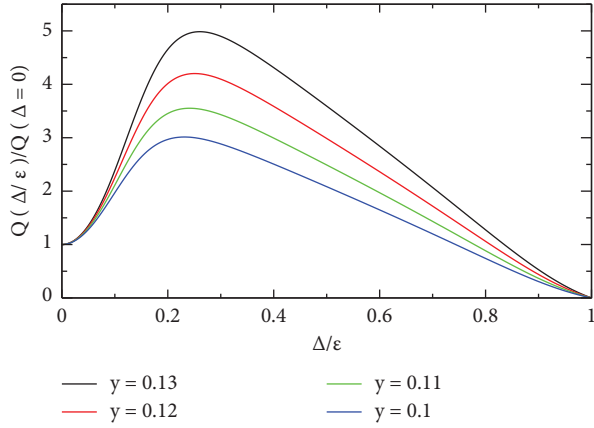


FIGURE 2: The ratio of total heat flux $(\dot{Q}_r(\Delta/\epsilon))/(\dot{Q}_r(\Delta=0))$ from the hot reservoir at a temperature T_r as a function of Δ/ϵ when $x = 0.99999$.

chemical potential to be identical in both reservoirs [3–5, 14, 15, 24].

3. Thermodynamic Properties of the Model

In this section, we evaluate and explore the behaviours of thermodynamic quantities such as heat flux and power as a function of a scaled energy parameter Δ/ϵ , which

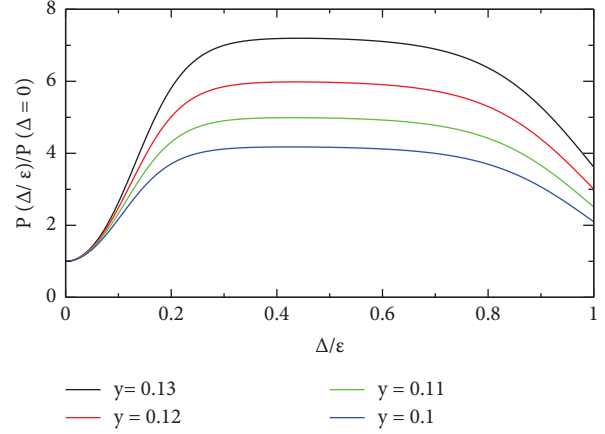


FIGURE 3: The net power output $(\dot{W}(\Delta/\epsilon))/\dot{W}(\Delta=0)$ that delivers from the quantum dots as a function of Δ/ϵ when $x = 0.99999$.

characterizes the energy difference between the two levels of the model.

3.1. Heat Flux. The rate of heat energy transferred through a given surface of a system can be described by the thermodynamic quantity, which is called heat flux. Substituting equations (2) and (6) into (10), the steady state heat per unit time as a function of Δ/ϵ becomes

$$\begin{aligned} \dot{Q}_r\left(\frac{\Delta}{\epsilon}\right) &= \alpha\epsilon\left(\left(\frac{\Delta}{\epsilon}\right)\left(\frac{1}{1+\exp(10(x+(\Delta/\epsilon)))}\right)\right. \\ &\quad \left.-\frac{1}{1+\exp(20(y+(\Delta/\epsilon)))}\right)+\left(-\frac{\Delta}{\epsilon}\right)\left(\frac{1}{1+\exp(10(x-(\Delta/\epsilon)))}\right) \\ &\quad \left.-\frac{1}{1+\exp(20(y-(\Delta/\epsilon)))}\right), \end{aligned} \quad (20)$$

where $x = 1 - \mu_r/\epsilon$, $y = 1 - \mu_l/\epsilon$.

The steady state heat per unit time with $\Delta = 0$ becomes

$$\dot{Q}_r(\Delta=0) = 2\alpha\epsilon x \left[\frac{1}{1+\exp(20x)} - \frac{1}{1+\exp(20y)} \right]. \quad (21)$$

The scaled heat per unit time of the thermodynamic quantity $((\dot{Q}_r(\Delta/\epsilon))/(\dot{Q}_r(\Delta=0)))$ can be exploited in Figure 2 as a function of Δ/ϵ . Figure 2 depicts the ratio of total heat flux as a function of Δ/ϵ . The heat flux getting into

the quantum dots increases when y increases. This means that when y increases, the chemical potential μ_l decreases. If x and y are comparable, this means that the chemical potentials μ_l and μ_r are equal and the power output will be zero. We note that μ_l is different from μ_r since the thermoelectric engine operates under an irreversible process.

3.2. Power. The steady state work per unit time (power) as the function of Δ/ϵ is given by

$$\begin{aligned}
\dot{W}\left(\frac{\Delta}{\epsilon}\right) = \alpha\epsilon & \left[\left(x + \frac{\Delta}{\epsilon} \right) \left[\frac{1}{1 + \exp((\epsilon/T_l)(x + (\Delta/\epsilon)))} \right. \right. \\
& - \left. \frac{1}{1 + \exp((\epsilon/T_l)(y + (\Delta/\epsilon)))} \right] + \left(x - \frac{\Delta}{\epsilon} \right) \left[\frac{1}{1 + \exp((\epsilon/T_l)(x - (\Delta/\epsilon)))} \right. \\
& - \left. \frac{1}{1 + \exp((\epsilon/T_l)(y - (\Delta/\epsilon)))} \right] - \left(y + \frac{\Delta}{\epsilon} \right) \left[\frac{1}{1 + \exp((\epsilon/T_l)(x + (\Delta/\epsilon)))} \right. \\
& - \left. \frac{1}{1 + \exp((\epsilon/T_l)(y + (\Delta/\epsilon)))} \right] - \left(y - \frac{\Delta}{\epsilon} \right) \left[\frac{1}{1 + \exp((\epsilon/T_l)(x - (\Delta/\epsilon)))} \right. \\
& \left. \left. - \frac{1}{1 + \exp((\epsilon/T_l)(y - (\Delta/\epsilon)))} \right] \right].
\end{aligned} \tag{22}$$

The steady state power when $\Delta = 0$ is given by

$$\dot{W}(\Delta = 0) = \alpha\epsilon \left[\frac{1}{1 + \exp(\epsilon x/T_r)} - \frac{1}{1 + \exp(\epsilon y/T_l)} \right] (2x - 2y). \tag{23}$$

The scaled net power output ($\dot{W}(\Delta/\epsilon)/\dot{W}(\Delta = 0)$) can be shown in Figure 3 as a function of Δ/ϵ .

In Figure 3, the scaled net power that delivers from the quantum dots increases when y increases. In general, the scaled input heat flux increases if the scaled net power output also increases. In Section 4, we study the efficiency at maximum power of the thermoelectric heat engine.

4. Thermoelectric Efficiency at Maximum Power

In this section, we determine the efficiency at maximum power of parallelly connected quantum dots (i.e., having the same dot energy) thermoelectric heat engine. To obtain the maximum power condition for a given temperature T_l and T_r , we search for the values of the scaled electron energy, i.e., the first derivative of power barriers x_l , x_r , y_l , and y_r that maximize \dot{W} becomes zero. We find the following four equations for both quantum dots. The first two equations corresponding to the first quantum dot are given by

$$\begin{aligned}
(f_l - f_r) + [(x_r - (1 - \eta_c)x_l]f_r^2 \exp(x_r) &= 0, \\
(f_l - f_r) + \left[\frac{x_r}{1 - \eta_c} - x_l \right] f_l^2 \exp(x_l) &= 0,
\end{aligned} \tag{24}$$

and the second two equations corresponding to the second quantum dot are given by

$$\begin{aligned}
(g_l - g_r) + [y_r - (1 - \eta_c)y_l]g_r^2 \exp(y_r) &= 0, \\
(g_l - g_r) + \left[\frac{y_r}{1 - \eta_c} - y_l \right] g_l^2 \exp(y_l) &= 0.
\end{aligned} \tag{25}$$

Equations (24) and (25) depend on the ratio of the two temperatures. From the two simultaneous equations

(equations (24) and (25)), we find a transcendental equation which is expressed as

$$x_l = 2 * \ln \left[\frac{\cosh(x_r/2)}{\sqrt{1 - \eta_c}} + \sqrt{\frac{\cosh^2(x_r/2)}{1 - \eta_c} - 1} \right] \tag{26}$$

$$y_l = 2 * \ln \left[\frac{\cosh(y_r/2)}{\sqrt{1 - \eta_c}} + \sqrt{\frac{\cosh^2(y_r/2)}{1 - \eta_c} - 1} \right]$$

and

$$\begin{aligned}
x_r - \sqrt{2} \cosh(x_r/2) \sqrt{2\eta_c - 1 + \cosh(x_r)} + 2(\eta_c - 1) \\
\times \ln \left[\frac{\cosh(x_r/2) + \sqrt{2\eta_c - 1 + \cosh(x_r)}/\sqrt{2}}{\sqrt{1 - \eta_c}} \right] \\
+ \sinh(x_r) = 0,
\end{aligned} \tag{27}$$

$$\begin{aligned}
y_r - \sqrt{2} \cosh(y_r/2) \sqrt{2\eta_c - 1 + \cosh(y_r)} + 2(\eta_c - 1) \\
\times \ln \left[\frac{\cosh(y_r/2) + \sqrt{2\eta_c - 1 + \cosh(y_r)}/\sqrt{2}}{\sqrt{1 - \eta_c}} \right] \\
+ \sinh(y_r) = 0,
\end{aligned} \tag{28}$$

respectively. Since an analytic solution of this equation is not possible, we first turn to perturbative solutions for η_c close to the limiting values 0 (reservoirs of equal temperatures) and 1 (cold reservoir at zero temperature) and also find the numerical values of x_l^{mp} and x_r^{mp} for any values of η_c . For the case $\eta_c \approx 0$, we substitute $x_r = a_0 + a_1\eta_c + a_2\eta_c^2 + \mathcal{O}(\eta_c^3)$ and $y_r = b_0 + b_1\eta_c + b_2\eta_c^2 + \mathcal{O}(\eta_c^3)$ in equations (27) and (28), respectively, and expand the resulting equation in η_c . The coefficients, $a_0, a_1, a_2, b_0, b_1, b_2$, and others, are found recursively by solving order by order in η_c . At order zero, we

find an identity. At the first order, we find the transcendental equations $a_0 = 2 \coth(a_0/2)$ and $b_0 = 2 \coth(b_0/2)$. The numerical solution is $a_0 = b_0 = 2.39936$. At second order and third order in η_0 , we find that $a_1 = b_1 = -a_0/4$ and $a_2 = b_2 = \sinh(a_0)/(b(1 - \cosh(a_0)))$. As we obtain from the perturbative solution, the values of $a_0 = b_0$, $a_1 = b_1$, and $a_2 = b_2$, then $x_r = y_r$ and the Fermi distribution becomes $f_r = g_r$ and $f_l = g_l$. Then, substituting all terms in equation (12) gets reduced into

$$\eta^{\text{mp}} = 1 - (1 - \eta_c) \frac{x_l^{\text{mp}}}{x_r^{\text{mp}}} = 1 - (1 - \eta_c) \frac{y_l^{\text{mp}}}{y_r^{\text{mp}}}. \quad (29)$$

The efficiency at maximum power in the regime of small η_c :

$$\eta^{\text{mp}} = \frac{\eta_c}{2} + \frac{\eta_c^2}{8} + \frac{31}{400}\eta_c^3 + \mathcal{O}(\eta_c^4). \quad (30)$$

Before we evaluate, numerically, let us define a dimensionless quantity τ which is the difference between the hot and cold reservoir temperature with respect to the cold reservoir, i.e.,

$$\tau = \frac{T_r - T_l}{T_l}. \quad (31)$$

From equations (27) and (28), we solve for the value of x_r^{mp} and y_r^{mp} for different values of τ numerically. Then, we find the corresponding value of x_l^{mp} and y_l^{mp} from equation (26). Finally, we substitute the values and we get for x_r^{mp} , y_r^{mp} , x_l^{mp} , and y_l^{mp} in equation (12) to find the efficiency at maximum power.

From Figure 4 which is the numerical solution for the efficiency at maximum power versus τ , we can observe that as τ goes to zero, the efficiency at maximum power becomes zero. This is because when τ becomes very small, the heat flux that is getting into the quantum dot becomes very small; hence, the efficiency is zero and as τ becomes large, the efficiency at maximum power approaches to one because as τ increases, the input power that the quantum dot receives increases which leads to an increase in efficiency.

We are solving the efficiency at maximum power as η_c runs from 0 to 1 numerically. First, we are solving the roots of equations (27) and (28) by varying η_c from 0 to 1 and substituting the values into equation (26) to find x_l and y_l . Then, we substitute all values into equation (12), and finally, we get Figure 5. Figure 5 shows that the efficiency at maximum power increases monotonically when we drive out of equilibrium. It is bounded from above by Carnot efficiency η_C , while the Curzon–Ahlborn efficiency η_{CA} provides a rather tight lower bound. The deviation between efficiency at maximum power and the Curzon–Ahlborn efficiency observes the values of η_c which goes to the maximum value.

5. Summary and Conclusion

In this work, we have taken a simple model of single-level two quantum dots connected between two heat reservoirs working as a heat engine. The model's simplicity enabled us to get analytic solutions for important quantities, such as efficiency at

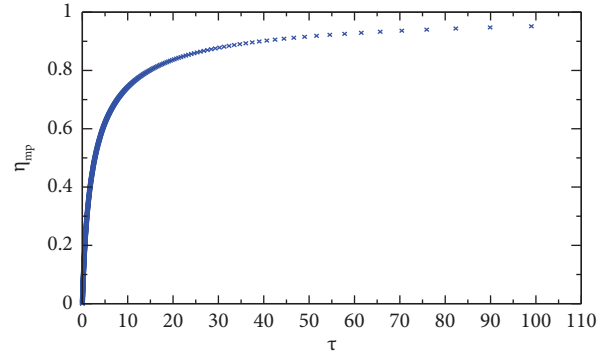


FIGURE 4: The plot of numerical value for efficiency at maximum power versus τ .

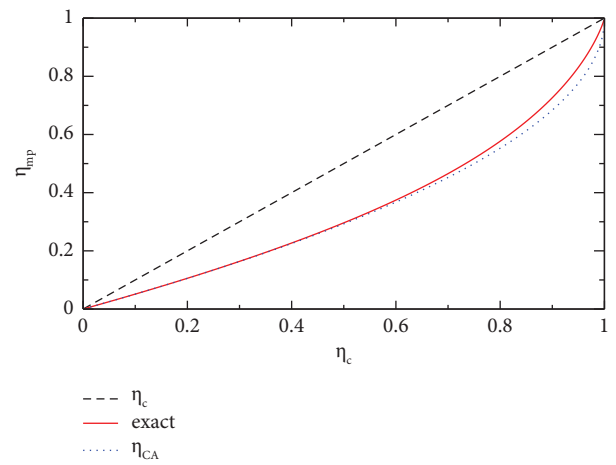


FIGURE 5: Efficiency at maximum power.

maximum power. To analyse the way energy is utilized by the engine, we started from the master equation and derived the efficiency, η , for the heat engine by first evaluating the heat flux extracted from the hot reservoir, \dot{Q}_r , heat flux dissipated into the cold reservoir, \dot{Q}_l , and delivered by the quantum dot. Maximizing the efficiency with respect to our power, \dot{W} , free parameters are the scaled electron energy barriers, x_r , x_l , y_r , and y_l . The efficiency at maximum power is evaluated by two approaches such as analytical solution and numerical solution. When the temperature of thermal reservoirs gets closer to each other, the coefficient of the linear term for the efficiency at maximum power is 1/2.

In conclusion, since the quantum dots are connected in parallel, the resulting efficiency at maximum power is the same as that obtained from one quantum dot. This model introduces another transport mechanism that prevents the energy conversion of thermoelectric devices.

Data Availability

No data were used to support the findings of this study.

Conflicts of Interest

The authors declare that they have no conflicts of interest.

Authors' Contributions

TB and MB conceptualized and prepared the design of the model. TB performed the analytic calculations. TB and YB performed the numerical simulations. TB, YB, YA, and MB analysed and interpreted the results. TB, YB, YA, and MB drafted the manuscript. All authors reviewed the results and approved the final version of the manuscript.

Acknowledgments

TB would like to thank the University of Gondar and Addis Ababa University for material support during our research work. We would also like to thank the International Science Programme, Uppsala University, Sweden, for the support they have provided to our research group.

References

- [1] F. L. Curzon and B. Ahlborn, "Efficiency of a Carnot engine at maximum power output," *American Journal of Physics*, vol. 43, no. 1, pp. 22–24, 1975.
- [2] H. B. Callen, *Thermodynamics and an Introduction to Thermostatistics*, John Wiley & Sons, Hoboken, NJ, USA, 2nd edition, 1985.
- [3] C. Van den Broeck, "Thermodynamic efficiency at maximum power," *Physical Review Letters*, vol. 95, no. 19, Article ID 190602, 2005.
- [4] B. Jiménez de Cisneros and A. C. Hernández, "Collective working regimes for coupled heat engines," *Physical Review Letters*, vol. 98, no. 13, Article ID 130602, 2007.
- [5] A. Gomez-Marin and J. M. Sancho, "Tight coupling in thermal Brownian motors," *Physical Review A*, vol. 74, no. 6, Article ID 062102, 2006.
- [6] T. Schmiedl and U. Seifert, "Efficiency at Maximum Power: An Analytically Solvable Model for Stochastic Heat Engines," *EPL (Europhysics Letters)*, vol. 81, no. 2, p. 20003, 2008.
- [7] Z. Tu, "Efficiency at maximum power of Feynman's ratchet as a heat engine," *Journal of Physics A: Mathematical and Theoretical*, vol. 41, no. 31, Article ID 312003, 2008.
- [8] M. Esposito, K. Lindenberg, and C. Van den Broeck, "Thermoelectric efficiency at maximum power in a quantum dot," *Institute of Science*, vol. 85, no. 6, Article ID 60010, 2009.
- [9] G. Snyder and E. Toberer, "Complex thermoelectric materials," *Nature Materials*, vol. 7, no. 2, pp. 105–114, 2008.
- [10] A. Majumdar, "Thermoelectricity in sn," *Science*, vol. 303, no. 5659, pp. 777–778, 2004.
- [11] A. I. Boukai, Y. Bunimovich, J. Tahir-Kheli, J. K. Yu, W. A. Goddard, and J. R. Heath, "Silicon nanowires as efficient thermoelectric materials," *Nature*, vol. 451, no. 7175, pp. 168–171, 2008.
- [12] J. P. Small, K. M. Perez, and P. Kim, "Modulation of thermoelectric power of individual carbon nanotubes," *Physical Review Letters*, vol. 91, no. 25, Article ID 256801, 2003.
- [13] P. Reddy, S. Y. Jang, R. A. Segalman, and A. Majumdar, "Thermoelectricity in molecular junctions," *Science*, vol. 315, no. 5818, pp. 1568–1571, 2007.
- [14] T. Humphrey, R. Newbury, R. Taylor, and H. Linke, "Reversible quantum brownian heat engines for electrons," *Physical Review Letters*, vol. 89, no. 11, Article ID 116801, 2002.
- [15] T. Humphrey and H. Linke, "Reversible thermoelectric nanomaterials," *Physical Review Letters*, vol. 94, no. 9, Article ID 096601, 2005.
- [16] T. B. Tegegne, *Thermodynamic properties of two quantum dots connected in parallel*, Ph.D. Thesis, Addis Ababa University, Addis Ababa, Ethiopia, 2012.
- [17] E. Bonet, M. M. Deshmukh, and D. Ralph, "Solving rate equations for electron tunneling via discrete quantum states," *Physical Review B*, vol. 65, no. 4, Article ID 045317, 2002.
- [18] D. Bagrets and Y. V. Nazarov, "Full counting statistics of charge transfer in Coulomb blockade systems," *Physical Review B*, vol. 67, no. 8, Article ID 085316, 2003.
- [19] U. Harbola, M. Esposito, and S. Mukamel, "Quantum master equation for electron transport through quantum dots and single molecules," *Physical Review B*, vol. 74, no. 23, Article ID 235309, 2006.
- [20] J. Schnakenberg, "Network theory of microscopic and macroscopic behavior of master equation systems," *Reviews of Modern Physics*, vol. 48, no. 4, pp. 571–585, 1976.
- [21] L. Jiu, C. Van den Broeck, and G. Nicolis, "Stability criteria and fluctuations around nonequilibrium states," *Zeitschrift für Physik B: Condensed Matter*, vol. 56, no. 2, pp. 165–170, 1984.
- [22] U. Seifert, "Entropy production along a stochastic trajectory and an integral fluctuation theorem," *Physical Review Letters*, vol. 95, no. 4, Article ID 040602, 2005.
- [23] M. Esposito, U. Harbola, and S. Mukamel, "Entropy fluctuation theorems in driven open systems," *Physical Review E*, vol. 76, no. 3, Article ID 031132, 2007.
- [24] C. Van den Broeck, "Carnot Efficiency Revisited," *Advances in Chemical Physics*, vol. 135, p. 189, 2007.